

## FUNDAMENTALS OF RIDGE CREST TOPOGRAPHY

E.E. DAVIS and C.R.B. LISTER

*Geophysics Group and Department of Oceanography, University of Washington, Seattle, Wash. (USA)*

Received August 30, 1973

Revised version received December 21, 1973

A linear relationship between the sea floor depth and the square root of age has been found for ocean lithosphere spreading from mid-ocean ridges. The asymptotic solution of depth as a function of age for the thermally contracting lithosphere predicts a linear dependence of depth on  $\sqrt{t}$  with a proportionality involving the initial lithosphere temperature, the thermal diffusivity, and the isostatic expansion coefficient averaged to include any temperature dependent phase changes. Empirical depth observations, when plotted as a function of the square root of age, bear out this prediction well, but there is a variation in the gradient,  $h/\sqrt{t}$ , along the ridge on a fine scale (up to 20% over 200 km). This implies a fundamental variation of the contraction parameter over the same scale, most probably of compositional origin. Details of a more complete cooling model near the ridge crest, including a crust of different thermal parameters than those of the mantle, predict a crestal height about 0.2 km below that of the simplified model. Individual profiles from the southeast Pacific show no such crestal deviation, and it is concluded that by quickly cooling the new crust, hydrothermal circulation may remove any effects of the crust which would be seen in the topography of a lithosphere cooled totally by conduction. The straightness of depth versus  $\sqrt{t}$  for older ocean data (to 80 m.y.) precludes any basal isothermal boundary shallower than 100 km.

### 1. Introduction

Several attempts have been made to model mid-ocean ridge topography by thermal contraction of the spreading oceanic lithosphere [1–8]. In most cases, unnecessary details in the models have served to obscure the fundamental behavior of the ridge crest topography with respect to the thermal properties of the material. Parker and Oldenburg [8] have taken a major step toward examining the fundamentals of thermally produced topography and find their solution quickly approaches a simple asymptotic relationship with time away from the ridge crest. In this paper we will follow a natural progression of steps in analyzing the thermal nature of the lithosphere and the related topographic expression, beginning with a case which is oversimplified, but nonetheless provides valuable insight for further analysis.

“The lesson, still to be learnt by many, is that a clear understanding of relatively shallow processes must be obtained before the more subtle, deep-seated forces will be revealed.”

Parker and Oldenburg, 1973

### 2. Fundamentals of topographic behavior

In the first simplified model, the lithosphere is created at a vertical plane boundary which is fixed at temperature  $T_1$ . The upper boundary of the lithosphere at  $z = 0$  is kept at  $T = 0$ , and the material is allowed to cool to unlimited depth. The model ignores horizontal conductive heat transport and any latent heat carried by liquid phases. By moving the reference system with the spreading lithosphere such that  $x = Ut$ , the solution for the temperature becomes simply [9, p.59]:

$$T = T_1 \operatorname{erf}(z/2\sqrt{kt})$$

The topographic anomaly due to the thermal expansion of this material is:

$$\begin{aligned} h &= \alpha_{\text{eff}} \int_0^{\infty} \{T_1 - T(z)\} dz \\ &= (2/\sqrt{\pi}) \alpha_{\text{eff}} T_1 \sqrt{kt} \end{aligned}$$

where  $\alpha_{\text{eff}}$  is the effective thermal expansion coefficient, modified for isostatic equilibrium, and can be written:

$$\alpha_{\text{eff}} = \frac{\rho_0}{\rho_0 - \rho_w} \alpha$$

if  $\rho_0$  = initial density, not a function of depth,  $\rho_w$  = water density,  $\alpha$  = thermal expansion coefficient, and  $\kappa$  = thermal diffusivity. The result shows that the topographic height is a linear function of  $\sqrt{t}$  with a proportionality constant of  $(2\sqrt{\pi})\alpha_{\text{eff}}T_0\sqrt{\kappa}$ . Thus we might expect that any plot of topography versus  $\sqrt{t}$  would produce a straight line in a region where the simplified model is applicable.

Let us now examine a more general situation in which we allow temperature dependence of the thermal parameters and phase changes. The full equation for constant initial temperature on a vertical boundary is given by Sclater and Francheteau [1]:

$$\rho C_p U \frac{\partial T}{\partial x} = K \left( \frac{\partial^2 T}{\partial x^2} + \frac{\partial^2 T}{\partial z^2} \right) + H \tag{1}$$

which can be rewritten as:

$$\frac{1}{l_0} \frac{\partial T}{\partial x} = \frac{\partial^2 T}{\partial x^2} + \frac{\partial^2 T}{\partial z^2} \tag{2}$$

for the case of zero heat generation and constant  $C_p$  (specific heat) and  $K$  (conductivity), where  $l_0 = K/\rho C_p U$  is the characteristic delay length for the flow. For a boundary layer with constant surface temperature, all temperature gradients become small as time and  $x = Ut$  increases. In fact, as Parker and Oldenburg [8] have pointed out, the solution is asymptotic to the one-dimensional cooling case (considered above) with  $t = x/U$ . Therefore, as  $T$  decreases monotonically with increasing  $x$  at constant  $z$ , the first term on the right hand side of eq. 2 becomes negligible compared to the left hand side, and the asymptotic solution satisfies the simplified equation:

$$\frac{1}{l_0} \frac{\partial T}{\partial x} = \frac{\partial^2 T}{\partial z^2}$$

Now in general,  $l_0$  is not really a constant, since both specific heat and conductivity vary somewhat with temperature. Further, there may be mineral rearrangements (phase changes) when a rock is cooled slowly. These changes may liberate, or even absorb latent heat, but provided they are not depth sensitive, they may be handled by the generalization of  $l_0$  to  $l(T)$ . We may then write the more general equation:

$$\frac{1}{l(T)} \frac{\partial T}{\partial x} = \frac{\partial^2 T}{\partial z^2}$$

and with the simple substitution:

$$T = \theta(z/\sqrt{x})$$

obtain:

$$-\frac{1}{2} \frac{1}{l(\theta)} \frac{z}{x^{3/2}} \theta' \left( \frac{z}{\sqrt{x}} \right) = \frac{1}{x} \theta'' \left( \frac{z}{\sqrt{x}} \right)$$

or

$$-\frac{1}{2} \frac{1}{l(\theta)} \xi \theta'(\xi) = \theta''(\xi)$$

where  $\xi = z/\sqrt{x}$ . Whatever solution this equation has, it is a function of  $\xi$  only and its form is time (and distance) invariant. The isostatically compensated topographic height, at constant initial density  $\rho_0$ , is given by:

$$\begin{aligned} \rho_0 l &= \rho_w h + \int_h^l \rho(T) dz \\ &= \rho_w h + \rho_0 l - \rho_0 h + \int_h^l (\rho - \rho_0) dz \\ h &= \frac{1}{\rho_0 - \rho_w} \int_h^l (\rho - \rho_0) dz \simeq \frac{1}{\rho_0 - \rho_w} \int_0^\infty (\rho - \rho_0) dz \end{aligned}$$

since the thermal equation has to ignore the distortion of the frame of reference producing  $h$ , and the compensation depth  $l$  is defined as deep enough for a negligible temperature change to be present. Now, provided that  $\rho$  is a function of temperature only, that is, not modified by pressure, it is a function of  $\xi$ , and  $\sqrt{x} d\xi = dz$ , so:

$$h = \frac{\sqrt{x}}{\rho_0 - \rho_w} \int_0^\infty [\rho(\xi) - \rho_0] d\xi$$

Whatever the details of the relation between  $\rho$  and  $T \equiv \theta$ , and the relation between  $\theta$  and  $\xi$ , the integral is a definite integral with the dimensions of density times square root of length. Hence:

$$h = \frac{\sqrt{x} \rho_0 \sqrt{L}}{\rho_0 - \rho_w} ,$$

and even in this rather general case, plots of topographic height against the square root of distance or time should be asymptotic to straight lines.

3. Topographic observations

Topographic data from Sclater et al. [4] for the Pacific, Atlantic, and Indian oceans are plotted against  $\sqrt{t}$  in Fig. 1. All sets of data show remarkably good fits to straight lines as predicted by the discussion above. The slopes give only the product of  $(2/\sqrt{\pi}) \alpha_{\text{eff}} T_1 \sqrt{\kappa}$ , modified by effects of phase changes and temperature dependence of the parameters, but for the sake of example we have assigned reasonable values as follows:

$$\rho_0 = 3.3 \text{ g cm}^{-3}$$

$$\alpha = 4.0 \times 10^{-5} \text{ } ^\circ\text{C}^{-1}$$

$$\kappa = 8.0 \times 10^{-3} \text{ cm}^2 \text{ sec}^{-1}$$

With these assumed values we obtain values of  $T_1$  for the data sets in Fig. 1: East Pacific Rise (North and South Pacific Ocean),  $T_1 = 1120 \text{ } ^\circ\text{C}$ ; Mid-Atlantic Ridge (South Atlantic Ocean), Central Indian Ridge, Carlsberg Ridge (Indian Ocean),  $T_1 = 1220 \text{ } ^\circ\text{C}$ . It is only speculation that this is the actual source of the differences in slope, but nevertheless both values are reasonable in light of experimental melting studies [10], and of observed basaltic magma eruptions and temperatures estimated by plagioclase geothermometry [11].

The slopes of  $h/\sqrt{t}$  do not decrease out to the time of the oldest topographic data, and this sets a minimum limit on the depth of any horizontal isothermal boundary.

Fig. 1 A. Averaged ocean depth versus the square root of age plotted for the Pacific Ocean (all points taken from Sclater et al. [4]). Depths are plotted relative to the crestal depth with the scale in 1-km divisions. Error bars show the standard deviation of the individual depth averages. The crestal intercept is defined as the intersection of the line fitted to the flank data with the time origin; crestal deviation is defined as the difference between the crestal intercept and the actual crestal depth.

Figure symbols are as follows:  $\circ$  = East Pacific Rise (North Pacific),  $\square$  = East Pacific Rise (South Pacific,  $< 3 \text{ cm/yr}$ ),  $\triangle$  = East Pacific Rise (South Pacific,  $> 3 \text{ cm/yr}$ ).

B. Averaged ocean depth versus the square root of age plotted for the Indian Ocean. Figure symbols are as follows:  $\circ$  = Carlsberg Ridge,  $\square$  = Southeast Indian Ridge,  $\triangle$  = Central Indian Ridge.

C. Averaged ocean depth versus the square root of age plotted for the South Atlantic Ocean. Slopes, crestal deviations, and spreading rates for all profiles are given in Table 1.

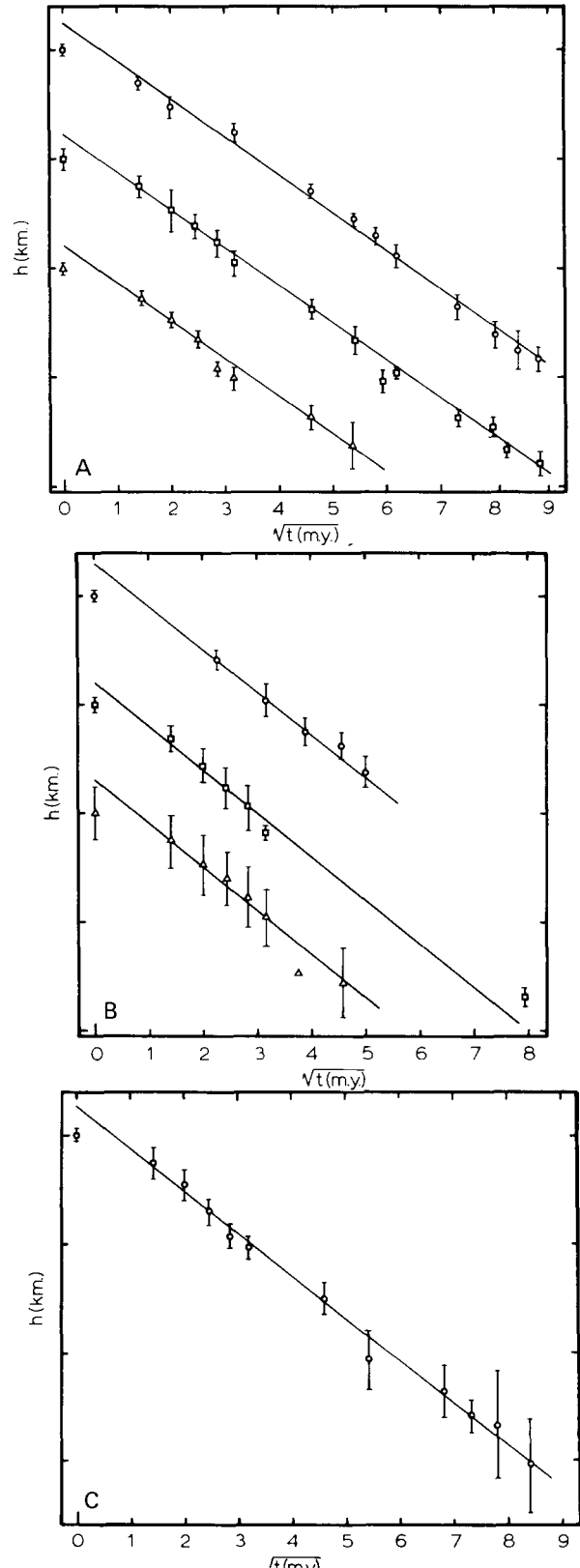


TABLE 1

Spreading rates, slopes of depth versus  $\sqrt{t}$ , and crestal deviations for averaged and individual depth profiles of Figs. 1 and 4. (All depths are taken at prominent magnetic anomalies.)

Profile location	Spreading rate (cm/yr)	Age range (m.y.)	$\Delta h/\sqrt{t}$ (km/ $\sqrt{\text{m.y.}}$ )	Crestal deviation (km)
<i>Averaged profiles</i>				
East Pacific Rise, North Pacific	$\sim 5^*$	78	0.35	0.25
East Pacific Rise, South Pacific	$< 3^*$	78	0.35	0.20
East Pacific Rise, South Pacific	$> 3^*$	29	0.35	0.20
Carlsberg Ridge	1.2	25	0.39	0.30
Southeast Indian Ridge	3.0	63	0.39	0.20
Central Indian Ridge	2.2	21	0.39	0.30
Mid-Atlantic Ridge, South Atlantic	2.0	71	0.39	0.25
<i>Individual Profiles (East Pacific Rise)</i>				
36° S east flank	direct dating	7.5	0.40	0
38° S east flank		8.5	0.52	0
40° S east flank		8.5	0.35	0
40° S west flank		7.5	0.35	0
42° S east flank		7.5	0.41	0
43° S east flank		10.0	0.40	0.05
43° S west flank		10.0	0.40	0.05
45° S east flank		10.0	0.33	0.05
45° S west flank		6.0	0.33	0.05
50° S west flank		7.5	0.51	0.05

\* Spreading rates vary between profiles averaged.

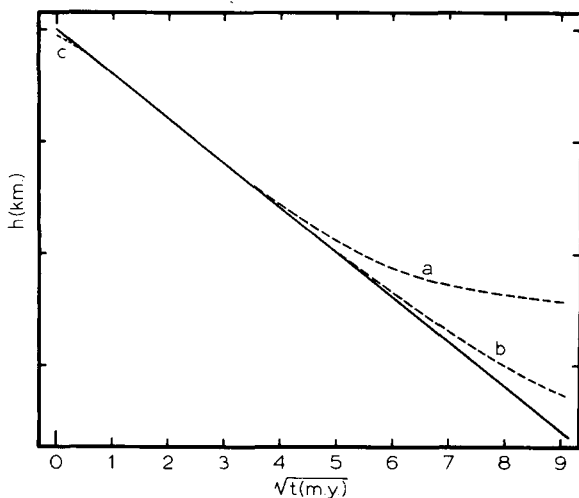


Fig. 2. The effects of imposing a horizontal isothermal boundary at 70 and 100 km are shown in curves (a) and (b) respectively. Curve (c) shows the result of the topographic solution including horizontal heat transport and using a thermal balance boundary condition at the ridge crest. The crestal deviation from the simple asymptotic solution is 50 m. All solutions (a, b and c) use the parameters of  $\alpha = 4.0 \times 10^{-5} \text{ } ^\circ\text{C}^{-1}$ ,  $\kappa = 0.008 \text{ cm}^2 \text{ sec}^{-1}$ , and  $T_1 = 1220^\circ\text{C}$  which produce a slope  $(2/\sqrt{\pi})\alpha_{\text{eff}} T_1 \sqrt{\kappa} = 0.39 \text{ km}/\sqrt{\text{m.y.}}$  to match data from the Indian and South Atlantic Oceans (see Fig. 1 and Table 1).

Shown in Fig. 2 are the results of imposing an isothermal boundary at 70 and 100 km depth as was done in the models of McKenzie [12], McKenzie and Sclater [13], Sclater and Francheteau [1], ect. The empirical data precludes a 70 km thick lithosphere and suggests that cooling is not limited even at 100 km.

One further consequence of the straightness of the empirical  $h/\sqrt{t}$  curves is that it provides a new and independent consistency argument for the linearity of the magnetic anomaly time scale, although an absolute calibration is not possible. That is, if either the magnetic chronology or the topographic model were wrong they would both have to be sympathetically in error to produce a straight line  $h/\sqrt{t}$  curve.

#### 4. Empirical $h/\sqrt{t}$ variation

Since there is a noticeable variation from ocean to ocean in the slope  $h/\sqrt{t}$ , it is important to test whether there is a variation on a finer scale. The empirical depth curves from Sclater et al. [4] have been averaged over large sections of ocean, and the standard deviations of the individual averaged depths are rather large. Some

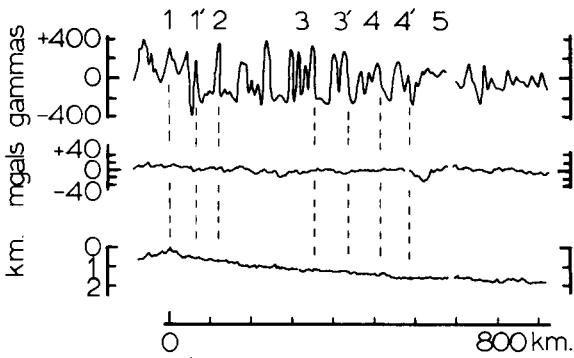


Fig. 3. A profile at 38°S exemplifying the smooth topography and well-defined magnetics of East Pacific Rise from which data were taken for Fig. 4. Magnetics are shown in gammas, free-air anomaly in mgals, and depth below the crest in km. Magnetic anomalies at depth sampling sites are numbered and distance from the crest is given. Only clear magnetic anomalies were used for assembling Fig. 4. Thus the plots are independent of complications due to fracture zone crossings or ridge crest jumps.

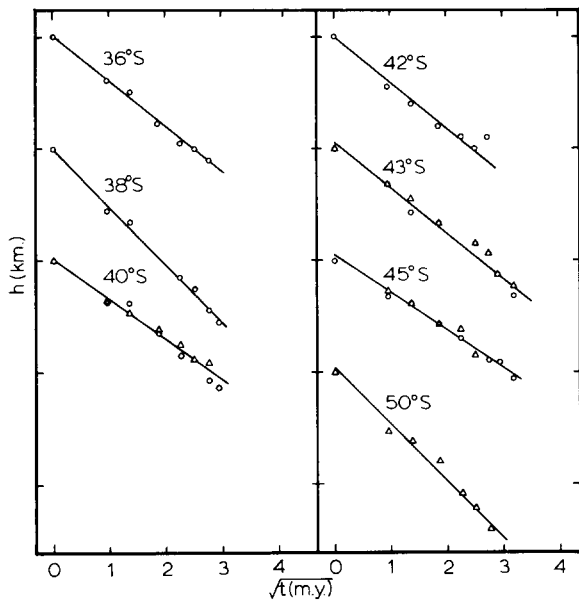


Fig. 4. Ocean depth versus the square root of age for individual profiles on the East Pacific Rise. Raw data for 38°S are shown in Fig. 3. Depths are plotted relative to the crestal depth with scale in 1-km divisions. As in Fig. 1, straight lines have been fitted through the data. Slopes and crestal deviations are listed in Table 1. Circles and triangles denote east and west flank data, respectively. Data sources: 40°S, 45°S [21]; 36°S, 50°S [22]; 43°S [23]; 38°S, 42°S [24].

of this deviation may be due to real slope variation as well as topographic “noise”.

To examine this possibility, we have chosen topographic data from the southeast Pacific from profiles whose topography is smooth and whose magnetic anomaly patterns are clearly defined. An example is shown in Fig. 3. The data from these are plotted again in the form of  $h$  versus  $\sqrt{t}$  in Fig. 4. The results show a large variation in slope (as much as 20% in just 2° latitude along the crest), but each individual profile falls very closely on a straight line. Data available from opposite flanks of the crest along individual lines (roughly perpendicular to the crestal axis) yield identical slopes. Therefore, there is good reason to believe that the slope variation among profiles is real. Again, the source of the variation can only be speculated upon, but it is likely that several or all of the factors involved in determining the slope (i.e.  $T_1, \alpha, \kappa$ , temperature dependence of these, and phase changes) may be involved in the variation.

That there are differences in the fundamental behavior of the crestal topography over such a fine scale sheds doubt on the accuracy often assumed when using depth as a tool to determine the age of oceanic lithosphere (e.g. Sclater, et al. [4], Anderson and Sclater [19], Anderson and Davis [20]). To give an example, the age of the 10 m.y. old crust of 38°S (magnetically well-defined) would be predicted at more than 20 m.y. by the averaged curves used by previous authors (compare the North Pacific, Fig. 1, with 38°S, Fig. 4). Hence suitable caution must be used when applying depth data as an age predicting tool.

### 5. Crestal topography

Observed topography at the crests of ridges, as plotted in Fig. 1, deviates significantly from the straight lines fitted through the data. Crestal depths systematically fall below where linear extrapolation of the flank points would predict by about 0.2 km. However, none of the individual profiles from the southeast Pacific discussed in section 4 show significant crestal deviation. Ridge-crest depths in Fig. 4 all lie on or less than 0.05 km below the fitted straight lines. The low crestal depths of Fig. 1 may result from the way the depths were chosen, whereas the smooth profiles used in Fig. 4 leave little doubt that at least on this part of the East

Pacific Rise, the crestral deviation is negligibly small. In this section we shall discuss how deviations from simple one-dimensional conductive cooling near the ridgecrest will affect the topographic behavior there. The treatments are simplified, but they should provide a rough estimate of the amount of topographic crestral deviation to be expected from the conductive model.

An obvious contribution to the deviation arises from the significant horizontal conduction of heat near the ridgecrest, the amount of heat conducted away from the crest being available to expand the adjacent lithosphere. This expansion is not included in the simplified model above, and would tend to lower the relative position of the crest. Horizontal conduction has been accounted for in the thermal solution of McKenzie [12], and is found to produce about 40 m of relative crestral depression.

The spreading model of McKenzie is still incomplete, however, as it does not account for the basic convective nature of the accreting boundary. If heat is conducted away horizontally as well as convected by the new lithosphere, the boundary cannot remain at  $T_1$ . That is, there must be a balance of heat at the origin, not an indefinite supply as the earlier models require. Parker and Oldenburg [8] have treated this problem by supplying latent heat at the accreting boundary when a liquid phase condenses to a solid at the melting point isotherm. As the amount of melt is probably small relative to the amount of solid phase over the bulk of the accreting lithosphere, we have chosen to ignore the latent heat. Rather, we have chosen a simple but realistic boundary condition, one of convective and conductive heat balance. Following the solution of McKenzie [12] for the temperature distribution in a moving slab, we have:

$$T' = 1 + z' + \sum_{n=1}^{\infty} A_n \exp(\alpha_n x') \sin(n\pi z') \quad (3)$$

where

$$\alpha_n = R - \sqrt{R^2 + n^2 \pi^2}$$

$$R = \rho C_p U l / 2K$$

and where  $T = T_1 T'$ ,

$$x = lx',$$

$$z = lz',$$

$l$  is the lithosphere thickness, allowed to be arbitrarily deep, and  $T_1$  is the material supply temperature. The

boundary condition desired at  $x = 0$  will balance the total heat flux, convective plus conductive, from the origin with that convected at the supply temperature  $T_1$ :

$$-K \frac{\partial T}{\partial x} + \rho C_p U T = \rho C_p U T_1$$

This boundary condition implies a discontinuity between the supply temperature and the temperature at the origin. It reflects the fact that the accretion *must* be discontinuous in time near the surface to satisfy both the heat balance and the requirement of magma fluidity in any model ignoring vertical flow. Removing the dimensions, we have:

$$-\frac{K}{\rho C_p U l} \frac{\partial T'}{\partial x'} + T' = 1$$

or:

$$-\frac{1}{2R} \frac{\partial T'}{\partial x'} + T' = 1$$

With this we may solve for  $A_n$  in eq. 3:

$$1 = 1 - z' + \sum_{n=1}^{\infty} \left\{ A_n \sin(n\pi z') - \frac{A_n}{2R} \alpha_n \sin(n\pi z') \right\}$$

$$\begin{aligned} A_n \frac{A_n \alpha_n}{2R} &= 2 \int_0^1 z' \sin(n\pi z') dz' \\ &= \frac{2(-1)^{n+1}}{n\pi} \end{aligned}$$

$$\text{Thus: } A_n = 2(-1)^{n+1} / n\pi \left( 1 - \frac{\alpha_n}{2R} \right) \quad (4)$$

This temperature distribution (eq. 3 with  $A_n$  from eq. 4) may now be applied to the topography of thermal expansion in the normal way. The resulting topography is plotted in Fig. 2 with the same thermal parameters found to fit the asymptotic Atlantic Ocean case. Again, we have ignored any modification of the kernel ( $2/\sqrt{\pi} \alpha_{\text{eff}} T_1 \sqrt{k}$ ) by phase changes, or temperature dependent parameters. As expected, the relative height of the crest is lower than that predicted by the vertical cooling model, but by an amount of only 50 m. This is a mere 10 m more than the deviation produced by the McKenzie solution; likewise, any reasonable statement of the initial boundary conditions will probably yield only a similar small crestral deviation.

If the crust-mantle boundary consists of a chemical change of material, then it is likely that the thermal

parameters of the two layers of the lithosphere are somewhat different. This, in turn, will affect the temperature distribution and the contraction of this layered case, and could produce a sizeable crestal deviation. We may estimate such a deviation due to a contrast in the expansion coefficients in the following way: if we assume a gabbroic composition (roughly 50% anorthite,  $\alpha = 2.0 \times 10^{-5}$ , and 50% pyroxene,  $\alpha = 3.2 \times 10^{-5}$  [17]) for the crust, we obtain an average value of  $\alpha = 2.6 \times 10^{-5}$  for the temperature range from 20°C to 800°C. A 5-km crust, completely cooled through 1200°C for example, will contract 0.24 km, whereas material having the same  $\alpha$  as used for the mantle,  $\alpha = 4.0 \times 10^{-5}$ , will contract 0.35 km. The resulting deviation is merely the difference between the two cases, or 0.1 km.

A rough estimate may also be obtained of the crestal deviation produced by a difference in thermal diffusivities between the crust and mantle. The diffusivity appears in the slope  $h/\sqrt{t} = (2/\sqrt{\pi}) \alpha_{\text{eff}} T_1 \sqrt{k}$ , and as an approximation, we will let the asymptotic slopes for the crust and mantle intersect at 1 m.y., a time in which a 5-km crust will be about 3/4 cooled, on average. Using reasonable values for diffusivity of  $6.7 \times 10^{-3}$  and  $8.0 \times 10^{-3}$  for the crust and mantle, respectively, we obtain a ratio in slopes of  $\sqrt{k(\text{crust})}/\sqrt{k(\text{mantle})} = 0.91$ . When applied from  $t = 1$  m.y. to the origin, the lower crustal slope will produce 45 m of crestal deviation.

The contributions from differences in thermal parameters for the crust and mantle and from a realistic boundary condition are additive, and when combined produce a total crestal deviation of about 0.2 km. Thus it becomes interesting that the individual profiles examined show no significant crestal deviation, and we are led to consider one further detail of the cooling of lithosphere.

All conductively cooled models suffer a common failure of not being able to account for the measured heat flow distribution over mid-ocean ridges. Heat flow values are far too low and scattered to justify a model whose lithosphere is cooled purely by conduction. This inability of conductive models to match the observed heat flow boundary condition is easily overcome if hydrothermal circulation takes place in the hot crust near the ridge crest. This process allows advection of heat directly from the crust, thereby reducing the conductive heat flow that is measured

through the surface. Hydrothermal activity has been suggested by several authors [16, 14], and the evidence has been summarized by Lister [14, 15]. The nature of the circulation, its depth of penetration, and its duration are not well understood; a simple first guess to determine its influence on heat flow was suggested by Lister [14], and this was used by Sclater and Klitgord [7] in their topographic model. This guess was one in which the hydrothermal circulation in the immediate vicinity of the crest established a linear gradient from zero temperature at the surface to  $T_1$  at the depth of its maximum penetration. Circulation quickly ceased away from the crest and cooling was purely conductive from that point onward.

A slightly more realistic representation of the initially cooled temperature distribution might be one in which the cooled layer was isothermally at the hot water temperature, a reasonable approximation if the water temperature is not too high. If the scatter and anomalously low values in heat flow are caused by hydrothermal activity as suggested by Talwani et al. [16] and Lister [14], then the data (e.g. Le Pichon and Langseth [2], fig. 4) would suggest that some circulation exists out to at least 40 m.y. A crustal layer in which convection continues would merely cause a nearly constant vertical offset in the shrinking topography of the lithosphere, since a slow reduction in the hydrothermal temperature as activity fades would cause a negligible height change. The mean initial temperature of the convecting layer is likely to be 200°C or less [15] and, because the rock is chilled and rigid, the applicable expansion coefficient should be closer to linear than volumetric. Complete cooling from 200°C to 0°C would cause a 5 km thick layer to shrink a mere 14 m. Hence we would expect no crestal deviation to be caused by continuing hydrothermal circulation in the crust; furthermore, the rapid convective cooling will obscure any topographic effects produced by contrasts between thermal parameters of the crust and mantle. Thus we would invoke this hydrothermal process to account for the lack of crestal deviation on the East Pacific Rise. Careful topographic study of other areas may show similar topographic behavior.

## 6. Conclusions

Sclater and Francheteau [1] have determined that the

general topography produced by sea-floor spreading systems can be accounted for by thermal contraction of the lithosphere as it spreads from its origin and cools from its initial temperature. By considering an oversimplified model of the oceanic lithosphere which allows cooling in the vertical direction only, a linear relationship between topography and the square root of time results, namely  $h = (2/\sqrt{\pi}) \alpha_{\text{eff}} T_0 \sqrt{\kappa t}$ . This relationship can be extended to a more generalized case where temperature dependence of the thermal parameters and temperature dependent phase changes are permitted as long as there is no significant variation with depth. Empirical sea floor topographic data follows a  $\sqrt{t}$  dependence rather closely.

From a detailed comparison between the empirical curves of depth versus  $\sqrt{t}$  and curves produced by calculation we can conclude:

(1) The oldest reliable topographic points do not show any of the curve flattening that would be caused by an isothermal boundary at depth, by significant internal heat generation, or by encroachment into the stability field of a major new rock mineral. More good data on the isostatic basement depth and age of older oceanic crust is needed if these phenomena are to be detected.

(2) There is a large variation in the slopes of closely spaced crestral profiles across the East Pacific Rise. The topographic data only extend out to 10 m.y., and may not reflect the long-time average slopes, but there is good reason to suppose that the variation is caused by changes in the slope parameter  $(2/\sqrt{\pi}) \alpha_{\text{eff}} T_1 \sqrt{\kappa}$ , presumably of compositional origin. Crustal age dating solely by means of absolute depth is therefore an unreliable tool.

(3) If the averaged depths from topographic data of Sclater et al. [4] are correct, then there is a deviation of the actual depth at the crest from the depth predicted by simplified theory. Such a deviation is expected if conductive cooling takes place in a crust and mantle whose thermal parameters vary. However, individual profiles from the southeast Pacific show no significant crestral deviation, and it is believed that hydrothermal circulation quickly cools the crust and removes the effects of different crustal parameters from the topography of the cooling lithosphere.

## Acknowledgement

This work was supported by grant GA 27947 of the National Science Foundation.

## References

- 1 J.G. Sclater and J. Francheteau, The implications of terrestrial heat flow observations on current tectonic and geochemical models of the crust and upper mantle of the earth, *Geophys. J.R. Astr. Soc.* 20 (1970) 509
- 2 X. Le Pichon and M.G. Langseth, Jr., Heat flow from the mid-ocean ridges and sea-floor spreading, *Tectonophysics* 8 (1969) 319.
- 3 N.H. Sleep, Sensitivity of heat flow and gravity to the mechanism of sea-floor spreading, *J. Geophys. Res.* 74 (1969) 542.
- 4 J.G. Sclater, R.N. Anderson and M.L. Bell, Elevation of ridges and evolution of the central eastern Pacific, *J. Geophys. Res.* 76 (1971) 7888.
- 5 D.W. Forsyth and F. Press, Geophysical tests of petrological models of the spreading lithosphere, *J. Geophys. Res.* 76 (1971) 1963.
- 6 P.W. Kasameyer, R.P. von Herzen, and G. Simmons, Heat flow, bathymetry, and the Mid-Atlantic Ridge at 43°N, *J. Geophys. Res.* 77 (1972) 2535.
- 7 J.G. Sclater and K.D. Klitgord, A detailed heat flow, topographic, and magnetic survey across the Galapagos spreading center at 86°W., *J. Geophys. Res.* 78 (1973) 6951
- 8 R.L. Parker and D.W. Oldenburg, Thermal model of ocean ridges *Nature* 242 (1973) 137.
- 9 H.S. Carslaw, and J.C. Jaeger, *Conduction of heat in solids*, (Oxford University Press, New York, 1959) 59, 2nd ed.
- 10 D.H. Green, Experimental melting studies on a model upper mantle composition at high pressure under water-saturated and water-under-saturated conditions, *Earth Planet. Sci. Lett.* 19 (1973) 37.
- 11 K.F. Scheidegger, Temperatures and compositions of magmas ascending along mid-ocean ridges, *J. Geophys. Res.* 78 (1973) 3340.
- 12 D.P. McKenzie, Some remarks on heat flow and gravity anomalies, *J. Geophys. Res.* 72 (1967) 6261.
- 13 D.P. McKenzie and J.G. Sclater, Heat flow in the eastern Pacific and sea-floor spreading, *Bull. Volcanol.* 33 (1969) 101.
- 14 C.R.B. Lister, On the thermal balance of a mid-ocean ridge, *Geophys. J.R. Astron. Soc.* 26 (1972) 515.
- 15 C.R.B. Lister, On the penetration of water into hot rock, submitted.
- 16 M.C. Talwani, C. Windisch and M.G. Langseth, Jr., Reykjanes ridge crest: a detailed geophysical study, *J. Geophys. Res.* 76 (1971) 473.

- 17 S.P. Clark Jr., Handbook of physical constants, G.S.A. Mem. 97 (1966).
- 18 K. Lambeck, Gravity anomalies over ocean ridges, Geophys. J. R. Astron. Soc. 30 (1972) 37.
- 19 R.N. Anderson, and J.G. Sclater, Topography and evolution of the East Pacific Rise between 5°S and 20°S, Earth Planet. Sci. Lett. 14 (1972) 433.
- 20 R.N. Anderson, and E.E. Davis, A topographic interpretation of the Mathematician ridge, Clipperton ridge, East Pacific Rise system, Nature 241 (1973) 191.
- 21 J.R. Heirtzler, D.E. Hayes, E.M. Herron and W.C. Pitman III, Preliminary report of Vol. 20, U.S.N.S. "Eltanin" cruises 16–21, Jan. 1965–Jan. 1966, Tech. Rep. 3–CU–3–69, Lamont-Doherty Geological Observatory of Columbia University, Palisades, New York (1969).
- 22 D.E. Hayes, J.R. Heirtzler, E.M. Herron and W.C. Pitman III, Preliminary report of Vol. 21, U.S.N.S. "Eltanin" cruises 22–27, Jan. 1966–Feb. 1967, Tech. Rep. 2–CV–2–69, Lamont-Doherty Geological Observatory of Columbia University, Palisades, New York (1969).
- 23 D.E. Hayes, M. Talwani, R. Houtz, W.C. Pitman III and R.R. Meijer II, Preliminary report of Vol. 22, U.S.N.S. "Eltanin" cruises 28–32, March 1967–March 1968, Tech. Rep. CU–1–72, Lamont-Doherty Geological Observatory of Columbia University, Palisades, New York (1972).
- 24 H.R. Stevens Jr., RP–1–OC–70, Southeast Pacific geophysical survey, NOAA Tech. Rep. ERL 261–POL–18 (1973).